

Lattice measurement of the couplings \hat{g}_∞ and $g_{B^*B\pi}$

A. ABADA^a, D. BEĆIREVIĆ^a, PH. BOUCAUD^a, G. HERDOIZA^{a,b}, J.P. LEROY^a,
A. LE YAOUANC^a, O. PÈNE^a

*Laboratoire de Physique Théorique (Bât.210), Université de Paris XI,
Centre d'Orsay, 91405 Orsay-Cedex, France.*

*Department of Physics, University of Wales Swansea,
Singleton Park, Swansea, SA2 8PP, United Kingdom.*

October 25, 2018

Abstract

We present the results of a quenched lattice QCD study of the coupling \hat{g} , in the static heavy quark limit. After combining this with our previous results obtained by using propagating heavy quarks with a mass around the physical charm quark, we are able to interpolate to the b -quark sector. Our results are $\hat{g}_\infty = 0.48 \pm 0.03 \pm 0.11$, $\hat{g}_b = 0.58 \pm 0.06 \pm 0.10$, and $g_{B^*B\pi} = 47 \pm 5 \pm 8$.

PACS: 12.38.Gc (Lattice QCD calculations), 13.75.Lb (Meson-meson interactions)

Introduction

The coupling of the vector and pseudoscalar heavy-light mesons to the pion, $g_{H^*H\pi}$, and the related \widehat{g}_Q defined through¹

$$g_{H^*H\pi} = \frac{2\sqrt{m_H m_{H^*}}}{f_\pi} \widehat{g}_Q, \quad (1)$$

have been extensively studied in the literature, both for phenomenological and theoretical reasons (a list of results can be found in refs. [1–5]). \widehat{g}_Q is particularly important in the studies of the q^2 -dependence of the form factor $F_+(q^2)$ which encodes the non-perturbative QCD dynamics of $D \rightarrow \pi$ and $B \rightarrow \pi$ semileptonic decays. To better illustrate this, we consider the dispersion formula for $F_+^{B \rightarrow \pi}(q^2)$:

$$F_+^{B \rightarrow \pi}(q^2) = \frac{1}{2m_{B^*}} \frac{f_{B^*} g_{B^*B\pi}}{1 - \frac{q^2}{m_{B^*}^2}} + \frac{1}{\pi} \int_{(m_\pi + m_B)^2}^{\infty} dt \frac{\text{Im}F_+(t)}{t - q^2 - i\varepsilon}, \quad (2)$$

where m_{B^*} and f_{B^*} are the mass and the decay constant of the B^* -meson. Near the B^* -pole, F_+ can be approximated by the first term of the r.h.s of eq. (2), which is why $g_{B^*B\pi}$ is so important. Inversely, from the q^2 -dependence deduced from the lattice data for $F_+^{B \rightarrow \pi}$, one can extract indirectly the value of $g_{B^*B\pi}$ (see e.g. [6]). Moreover the need for a more accurate estimate of \widehat{g}_Q became recently more evident since the guidance of the chiral extrapolations by the predictions of the heavy meson chiral perturbation theory necessarily involves \widehat{g}_Q [7]. In the effective theory based on the combination of the heavy quark and chiral symmetries [8, 9] one of the essential parameters is the coupling \widehat{g}_∞ which appears as the infinite quark mass limit of \widehat{g}_Q :

$$\widehat{g}_Q = \widehat{g}_\infty + \mathcal{O}(1/m_Q^n). \quad (3)$$

While the $B^* \rightarrow B\pi$ decay is forbidden by the lack of phase space and therefore the coupling $g_{B^*B\pi}$ cannot be measured in experiment, the coupling $g_{D^*D\pi}$ has already been measured. CLEO reported recently [10]:

$$g_{D^*D\pi} = 17.9 \pm 0.3 \pm 1.9, \quad (4)$$

$$i.e. \widehat{g}_c^{\text{exp.}} = 0.61 \pm 0.01 \pm 0.07, \quad (5)$$

where we used eq. (1) to obtain \widehat{g}_c from $g_{D^*D\pi}$. Since the pion emerging from this decay is soft, the experimental measurement of $\Gamma(D^{*+})$ is difficult. The experimental confirmation of the CLEO results would be highly welcome.

Regarding the theoretical estimates the situation is still quite unsatisfactory. Typical values for \widehat{g}_Q , as obtained by using the QCD sum rules (QCDSR) are low, around 0.3 [1], in disagreement with $\widehat{g}_c^{\text{exp.}}$. Such a disagreement with the experimental value was not, however, observed with similar couplings, such as $g_{\rho\omega\pi}$, $g_{NN\pi}$, or $g_{\Sigma_c^* \Lambda_c \pi}$. To overcome that problem, in ref. [11] it has been proposed to include the first radial excitations in the

¹The subscript $Q \in \{c, b\}$ refers to the heavy quark constituent of the heavy-light meson.

hadronic part of the sum rules, below the duality threshold. As a result the coupling \widehat{g}_c becomes much larger ($\widehat{g}_c \sim 0.7$), while the similar modification of the sum rule leaves the decay constants (f_D and f_{D^*}) unchanged.

Predictions of various quark models are in the range $0.3 \lesssim \widehat{g}_\infty \lesssim 0.8$ [12]. In particular, in the model with the Dirac equation a value of \widehat{g}_∞ around 0.6 was found before the experimental result became available [2]. On the lattice, a quenched calculation by UKQCD [13] led to $\widehat{g}_\infty = 0.42(4)(9)$. This exploratory study was carried out in the static heavy quark limit where the difficulties to isolate the ground state are well known. In addition it was performed on a coarse lattice, with a low statistics and with only two light quark masses from which it was extrapolated to the chiral limit. Finally, the indirect measurements using the lattice data for the form factors F_+ and F_0 [6] have extracted rather small values [6].

In our recent paper [4], we presented the results of the quenched lattice simulation in which we used the propagating heavy quarks with the mass around the physical charm quark. We obtained, $\widehat{g}_c = 0.67 \pm 0.08_{-0.06}^{+0.04}$, and observed no apparent dependence on the heavy quark mass. Actually the 3 values of \widehat{g}_Q measured directly in the neighbourhood of the c -quark mass were compatible within our error bars and shew only a very small negative slope (see section 4.3 of ref. [4]). This situation allowed a safe *interpolation* to the c -quark but the determination of \widehat{g}_∞ relied heavily on the hypothesis that the observed behaviour was valid over the whole mass-range. In order to check the validity of this assumption we have performed a lattice quenched computation of \widehat{g} In the static heavy quark limit, the outcome of which is presented in this paper. Our result is

$$\widehat{g}_\infty = 0.48 \pm 0.03 \pm 0.11 , \quad (6)$$

where the errors are statistical and systematic, respectively. Using this and the results we presented in ref. [4], we were able to interpolate to the b -quark. We get

$$\begin{aligned} \widehat{g}_b &= 0.58 \pm 0.06 \pm 0.10 , \\ g_{B^*B\pi} &= 47 \pm 5 \pm 8 . \end{aligned} \quad (7)$$

By comparing eqs. (6) and (7), our results suggest that the $1/m_B$ corrections to \widehat{g}_∞ are of the order of 20 – 30%.

The paper is organized as follows: after this introduction we explain in Sec. 1 the relation between \widehat{g} and the matrix elements that we compute on the lattice; in Secs. 2 and 3 we present the details of our lattice study and show our main results; Sec. 4 is devoted to the discussion of systematic errors; in Sec. 5 we interpolate to the physical B -meson mass; finally we summarize our findings in Sec. 6.

1 Extracting \widehat{g}_∞

The coupling $g_{H^*H\pi}$ (with $H \in \{D, B\}$) is defined by the matrix element

$$\langle H(p') \pi(q) | H^*(p, \lambda) \rangle = g_{H^*H\pi} (q \cdot \epsilon^\lambda(p)) , \quad (8)$$

where $q = p - p'$ and $\epsilon^\lambda(p)$ is the polarization of the vector meson. To determine $g_{H^*H\pi}$, we can consider the matrix element of the divergence of the light–light axial current,

$A_\mu = \bar{q}\gamma_\mu\gamma_5q$. In the limit where the pion is soft, we can write

$$\langle H(p')|q_\mu A^\mu|H^*(p, \lambda)\rangle = g_{H^*H\pi}\frac{q \cdot \epsilon^\lambda(p)}{m_\pi^2 - q^2} \times f_\pi m_\pi^2 + \dots \quad (9)$$

where the dots stand for terms suppressed when q^2 is small and close to the m_π^2 -pole. To bring out $g_{H^*H\pi}$ from (9) we express the l.h.s in terms of the form factors, $A_{0,1,2}$, evaluated on the lattice. The standard parametrization reads

$$\begin{aligned} \langle H(p')|A^\mu|H^*(p, \lambda)\rangle &= 2m_{H^*}A_0(q^2)\frac{\epsilon^\lambda \cdot q}{q^2}q^\mu + (m_{H^*} + m_H)A_1(q^2)\left[\epsilon^{\lambda\mu} - \frac{\epsilon^\lambda \cdot q}{q^2}q^\mu\right] \\ &+ A_2(q^2)\frac{\epsilon^\lambda \cdot q}{m_H + m_{H^*}}\left[p^\mu + p'^\mu - \frac{m_{H^*}^2 - m_H^2}{q^2}q^\mu\right]. \end{aligned} \quad (10)$$

Note that when $\vec{q} = \vec{0}$, the soft pion limit is verified, since $q^2 = (m_{H^*} - m_H)^2 \sim 0$. Moreover, if we choose $\vec{q} = \vec{0}$ and $\vec{p} = \vec{p}' = \vec{0}$, eq. (10) simplifies to

$$\langle H|A_i|H^*\rangle = (m_{H^*} + m_H)A_1(0)\epsilon_i^\lambda. \quad (11)$$

As discussed in our previous paper [4], when $q^2 = 0$ the form factors $A_{0,1,2}$ are related to one another because the q^2 -poles in eq. (10) are unphysical and therefore their residues have to cancel. This leads to the relation

$$2m_{H^*}A_0(0) = (m_{H^*} + m_H)A_1(0) + (m_{H^*} - m_H)A_2(0). \quad (12)$$

When taking the divergence of the axial current in (10), only the term in A_0 remains on the r.h.s. so that by using eq. (9), we arrive at

$$g_{H^*H\pi} = \frac{2m_{H^*}A_0(0)}{f_\pi} \quad (13)$$

$$= \frac{1}{f_\pi} [(m_{H^*} + m_H)A_1(0) + (m_{H^*} - m_H)A_2(0)]. \quad (14)$$

Finally, inserting the definition (1) leads to the expression for \widehat{g}_Q

$$\widehat{g}_Q = \frac{(m_{H^*} + m_H)}{2\sqrt{m_H m_{H^*}}}A_1(0) + \frac{(m_{H^*} - m_H)}{2\sqrt{m_H m_{H^*}}}A_2(0). \quad (15)$$

Owing to the heavy quark symmetry, the vector and the pseudoscalar heavy–light mesons are degenerate in the static limit and eq. (15) simply becomes

$$\widehat{g}_\infty = A_1(0). \quad (16)$$

Thus, the value of \widehat{g}_∞ (in the static heavy quark limit) is simply given by the form factor A_1 at $\vec{q} = \vec{0}$.

2 Strategy for the calculation of \widehat{g}_∞ on the lattice

To determine the form factor $A_1(0)$ from the lattice evaluation of the matrix element $\langle H | A^\mu | H^* \rangle$, we use eq. (11) where H and H^* now refer to the pseudoscalar and vector mesons containing an infinitely heavy quark. We consider the two- and three-point correlation functions, C_2 and $C_{3\mu\nu}$, with local (L) and smeared (S) interpolating fields for mesons consisting of a static heavy and a propagating light quarks.

In the case in which both the source and the sink are smeared, the two-point functions are defined as

$$C_2^{SS}(t_x) = \left\langle \sum_{\vec{x}} P^S(x) P^{S\dagger}(0) \right\rangle = \frac{1}{3} \sum_{i=1}^3 \left\langle \sum_{\vec{x}} V_i^S(x) V_i^{S\dagger}(0) \right\rangle, \quad (17)$$

where P^S and V_μ^S are the smeared interpolating fields of the pseudoscalar and vector mesons. $C_2^{SL}(t_x)$ is obtained by simply replacing $P^S \rightarrow P^L = \bar{q}\gamma_5 h$, $V^S \rightarrow V^L = \bar{q}\gamma_\mu h$, where h stands for the static heavy quark field. The equality between the pseudoscalar and vector meson correlation functions in eq. (17) is a consequence of the heavy quark symmetry. When the excited states are decoupled and the ground state isolated (at large enough t_x), the two-point function becomes

$$C_2^{SS}(t_x) = (\mathcal{Z}^S)^2 e^{-E_H^{SS} t_x}, \quad (18)$$

where E_H is the binding energy of the static heavy–light meson, and

$$\mathcal{Z}^S \equiv \frac{\langle 0 | P^S | H \rangle}{(2m_H)^{1/2}}. \quad (19)$$

The *three-point* Green functions with smeared interpolating fields are defined in the following way,

$$C_{3\mu\nu}^{SS}(0, t_x, t_y) = \left\langle \sum_{\vec{x}, \vec{y}} P^S(y) A_\nu(x) V_\mu^{S\dagger}(0) \right\rangle \Bigg|_{0 < t_x < t_y}, \quad (20)$$

where the vector and pseudoscalar mesons are inserted at the origin and at a fixed time t_y , respectively. The insertion time t_x of the (local) axial current ($A_\mu = \bar{q}\gamma_\mu\gamma_5 q$) varies in the range $0 - t_y$. The matrix element we are considering, $\langle H | A_\mu | H^* \rangle$, is then extracted from the following ratio:

$$\begin{aligned} R^{SS}(t_x) &= \frac{1}{3} \sum_{i=1}^3 \frac{C_{3i}^{SS}(t_x) \mathcal{Z}_S \mathcal{Z}_S}{C_2^{SS}(t_x) C_2^{SS}(t_y - t_x)} \\ &\rightarrow \frac{1}{3} \sum_{i=1}^3 \epsilon_i^\lambda(\vec{0}) \frac{\langle H | A_i(t_x) | H^* \rangle}{2m_H} \Bigg|_{0 \ll t_x \ll t_y} = A_1(0) = \widehat{g}_\infty. \end{aligned} \quad (21)$$

The time dependence cancels in the ratio, so that a plateau in time of $R^{SS}(t_x)$ directly leads to the value of $A_1(0)$, which for $m_q \rightarrow 0$ becomes the desired coupling \widehat{g}_∞ . In what

follows we will use the notation in which $A_1(0) \equiv \hat{g}_\infty$, even though this is strictly true only for $m_q \rightarrow 0$.

In our simulation we choose to work with the usual (improved) Wilson light quarks and with the static heavy quark by using the Eichten–Hill action [15]. In terms of quark propagators and the Wilson line, the three-point correlation function (20) can be written as

$$C_{3\mu\nu}^{LL}(t_x) = \left\langle \sum_{\vec{x}, \vec{y}} \text{Tr} \left[\frac{1 + \gamma_0}{2} P_y^0 \gamma_\mu S_u(0; x; U) \gamma_\nu \gamma_5 S_d(x; y; U) \gamma_5 \right] \right\rangle_U, \quad (22)$$

where $S_q(x; y; U) = q(x)\bar{q}(y)$ is the propagator of the light quark q . In our study the two light quarks are degenerate, $m_u = m_d \equiv m_q$. The brackets $\langle \dots \rangle_U$ indicate the average over the background gauge field configurations (U), whereas P_y^x is the ordered product of links in the time direction (Wilson line),

$$P_y^x = \delta(\vec{x} - \vec{y}) \prod_{t_z=t_x}^{t_y-1} U_t(x + t_z \hat{t}), \quad (23)$$

with \hat{t} being the unit vector in the time direction.

To improve the statistical quality of the signal we implement the recent proposal of ref. [17] and replace the simple link variables in the Wilson line by the so called “*fat links*”, defined as

$$U_t(x) \rightarrow U_t^{\text{fat}}(x) = \frac{1}{6} \sum_{i=x,y,z} \left[U_i^{\text{Staple}}(x, x + \hat{t}) + U_{-i}^{\text{Staple}}(x, x + \hat{t}) \right]. \quad (24)$$

In order to isolate the ground state from the correlators (22) at the smallest time separations, it is necessary to devise an efficient smearing procedure. We use the proposal of ref. [14] and replace the quark fields $q(x)$ by

$$q(x) \rightarrow \sum_{r=0}^{R_{\text{max}}} (r + \frac{1}{2})^2 \phi(r) \sum_{i=x,y,z} \left\{ \left[\prod_{k=1}^r U_i^F(x + (k-1)\hat{i}) \right] q(x + r\hat{i}) + \left[\prod_{k=1}^r U_i^{F\dagger}(x - k\hat{i}) \right] q(x - r\hat{i}) \right\}. \quad (25)$$

The wave function $\phi(r)$ is chosen in such a way that the overlap with the ground state is increased. We take $\phi(r) = e^{-r/R_b}$, where R_b is a parameter which is fixed by requiring that the smearing be optimal. Note that it is not necessary to normalize the wave function since the normalisation factors cancel in the ratio (21). The smearing also includes the so called fuzzing: the gauge links U^F are fuzzed by N_F iterations of the following procedure

$$U_j(x) \rightarrow U_j^F(x) = \mathcal{P} \left[C U_j(x) + \sum_{i \neq j} \left[U_i^{\text{Staple}}(x, x + \hat{j}) + U_{-i}^{\text{Staple}}(x, x + \hat{j}) \right] \right], \quad (26)$$

where \mathcal{P} is used to project the fuzzed fields onto $SU(3)$, and C is a real parameter.

3 Conditions and results of the simulation

The main results presented in this work are obtained from the simulation performed on a $24^3 \times 28$ lattice with periodic boundary conditions, at $\beta = 6.2$. We collect 160 independent $SU(3)$ gauge configurations in the quenched approximation. The Wilson fermion action is non-perturbatively $\mathcal{O}(a)$ improved with $c_{SW} = 1.614$ [18]. The light quark propagators are computed with the following Wilson hopping parameters:

$$\kappa_q = 0.1344_{q_1}, 0.1348_{q_2}, 0.1351_{q_3}, \quad (27)$$

corresponding to quark masses around the physical strange quark.

We will present our results using our preferred set of parameters, $t_y = 13a$, $R_{max} = 5a$, $R_b = 3.0a$, $N_F = 5$ and $C = 4$. The motivation for this choice of parameters, the effect of the smearing (25) and of the modification of the static heavy quark action (24), will be discussed in section 4, where we will also quantify the systematic effects involved in our calculation.

3.1 Study of the two-point functions

Light–light operator: The axial current appearing in eq. (20) consists of two light quarks. Even though we use the improved Wilson quarks, for our purpose there is no need to improve the bare axial current since the form factor A_1 is insensitive to the presence of the $\mathcal{O}(a)$ improvement term. On the other hand, the improvement of the renormalization constant is of course necessary. We use

$$Z_A^I(g_0^2) = Z_A^{(0)}(g_0^2) \left(1 + \tilde{b}_A(g_0^2) a \rho \right), \quad (28)$$

where the quark mass $a\rho$ is obtained from the axial Ward identity, $\partial_\mu A_\mu = 2\rho P$ ($P = \bar{q}\gamma_5 q$). The non-perturbatively evaluated renormalization constants are: $Z_A^{(0)} = 0.81(1)$ [19, 20] and $\tilde{b}_A = 1.19(6)$ [19] at $\beta = 6.2$. We have checked that the inverse lattice spacing obtained from the pion decay constant is consistent with the one we reported in our previous paper. Since the temporal extension of the lattice used in our previous paper is much larger than the present one we will use, whenever needed, $a^{-1}(f_\pi) = 2.71(12)$ GeV from ref. [4].

Static heavy–light correlators: The binding energy E_H and the constant \mathcal{Z} are obtained from the two-point correlation function as indicated in eq. (18). To identify the plateau in time where the ground state is properly isolated, we study the effective binding energy,

$$E_{\text{eff}}^{SS}(t) = \ln \left(\frac{C_2^{SS}(t)}{C_2^{SS}(t+1)} \right). \quad (29)$$

The superscript “ SS ” refers to the situation in which both interpolating fields are smeared. Note also that the projection $\frac{1+\gamma_0}{2}$ of the static quark onto the positive energy states reduces the contamination of the signal coming from the opposite side of the periodic lattice. Therefore, the time reversal symmetry over the time dimension of the lattice is not preserved in the heavy quark limit and the two-point functions are no longer symmetric

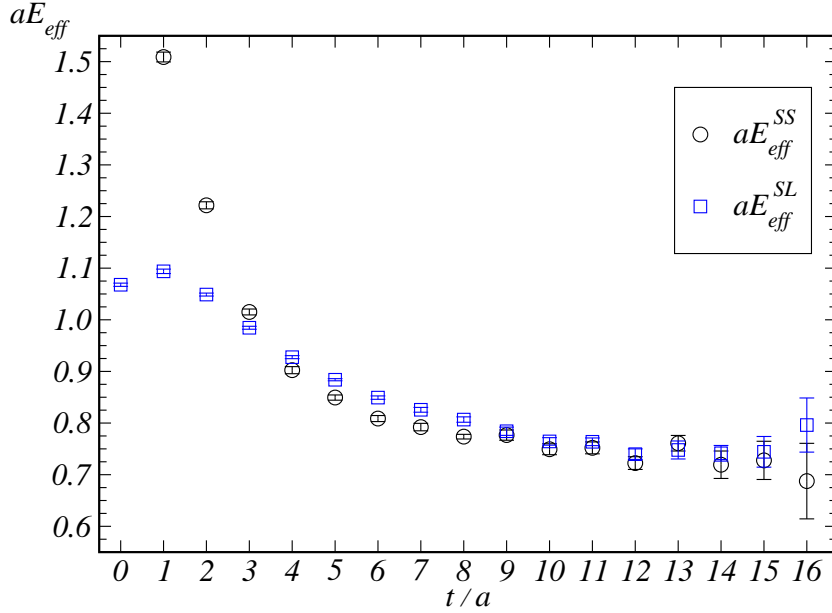


Figure 1: Signals for the effective binding energies obtained by using eq. (29) in case of Smeared-Smeared (“SS”) and Smeared-Local (“SL”) sources. In both cases the light quark mass corresponds to $\kappa_q = 0.1344$, whereas for the static quark we use the “fat” links as discussed in the text (see eq. (24)).

with respect to $t = T/2$. We illustrate in fig. 1 the signals for the effective binding energies of the C_2^{SS} and C_2^{SL} correlators. By fitting to the form (18) in the time interval in which the plateau is observed, we extract E_H and \mathcal{Z} . We have also considered a fit with two exponentials, but did not observe any noticeable effect. The double exponential fit becomes necessary only for when performing simulations without the “fattening” indicated in eq. (24) because in that case the plateaus of $E_{\text{eff}}(t)$ are much shorter.

We first calculate the B -meson decay constant, $f_{B_s}^{\text{static}}$. Rather than providing an accurate value for this quantity (a precision determination of $f_{B_s}^{\text{static}}$, has already been made in ref. [17]), our intention is only to test the validity of our computation. \mathcal{Z}^L is not obtained directly from the local–local correlators because the corresponding correlators are much less stable and statistically noisier than the smeared–local ones. For this reason \mathcal{Z}^L is extracted from

$$R_{\mathcal{Z}}(t) = \mathcal{Z}^S \times \frac{C_2^{SL}(t)}{C_2^{SS}(t)} \Big|_{t \gg 1} \rightarrow \mathcal{Z}^L. \quad (30)$$

In table 1, we present the values of E_H^{SS} , E_H^{SL} , \mathcal{Z}^S , and \mathcal{Z}^L for a static heavy quark and light quarks with masses corresponding to the κ_{q_i} ’s specified in eq. (27). The decay constant $f_{B_s}^{\text{static}}$ is obtained from \mathcal{Z}^L using $m_{B_s} = 5.37$ GeV, i.e. the physical B_s -meson mass,

$$f_{B_s}^{\text{static}} = Z_A^{\text{stat}} \mathcal{Z}^L \sqrt{\frac{2}{m_{B_s}}} a^{-3/2}, \quad (31)$$

	aE_H^{SS}	aE_H^{SL}	Z^S	Z^L
static- q_1	0.760(4)	0.758(4)	64.8 ± 2.3	0.126(3)
static- q_2	0.748(5)	0.745(5)	60.8 ± 2.4	0.121(3)
static- q_3	0.740(5)	0.737(6)	57.8 ± 2.5	0.117(3)

Table 1: *The values of the binding energies obtained by using the Smeared-Smeared and Smeared-Local two-point correlation functions. The corresponding constants Z^S and Z^L are also given (see eq. (18)). The time intervals chosen for the fits are: $t/a \in [8, 13]$ for E_H^{SS} , Z^S , and $t/a \in [9, 13]$ for E_H^{SL} , Z^L .*

and $Z_A^{stat} = 0.77(3)$, the static heavy-light axial current renormalization constant computed non-perturbatively in ref. [16]. Notice that this value of Z_A^{stat} is obtained by using the Eichten-Hill static heavy quark action, i.e. without including the effects of the fattening (24). In ref. [17], however, it has been argued, on the basis of the observed behaviour of the step scaling function, that the effect on Z_A^{stat} of the modification of the static quark action is only very small. Therefore the value we are using is certainly sufficient to achieve our present goal which, we recall, is to check the compatibility of our results with previous ones.

In fig. 2, we provide an illustration of the signal (plateau) of the ratio $R_z(t)$, and plot the corresponding $f_{B_q}^{static}$, as obtained by using eq. (31). From the linear interpolation to the strange quark mass (corresponding to $m_{ss}^2 = 2m_K^2 - m_\pi^2$), we obtain f_{B_s} , which we quote as

$$f_{B_s}^{static} = \frac{Z_A^{stat}}{0.77} (251 \pm 20 \text{ MeV}). \quad (32)$$

This value agrees quite well with the one, $f_{B_s}^{static} = 225 \pm 10 \text{ MeV}$, recently obtained also at $\beta = 6.2$, in ref. [17].

3.2 Study of the three-point functions

We observe that, for t_x not too close to 0 or t_y , the three-point function, $C_{3ii}^{SS}(0, t_x, t_y)$, introduced in eq. (20), does not depend on t_x . The reason for this is that, in the static limit, the ground states of the vector and pseudo-scalar mesons are degenerate. Therefore, by writing $C_{3ii}^{SS}(0, t_x, t_y)$ as

$$\sum_k \sum_l \langle 0 | P(t_y) | H_k \rangle \langle H_k | A_i(t_x) | H_l^* \rangle \langle H_l^* | V_i^\dagger(0) | 0 \rangle, \quad (33)$$

where k and l label the excitations, one sees that in the *diagonal* contribution ($k = l$) the exponential time dependence writes

$$e^{-(E_{H_l^*} - E_{H_k})t_x - E_{H_k}t_y} = e^{-E_{H_k}t_y}, \quad (34)$$

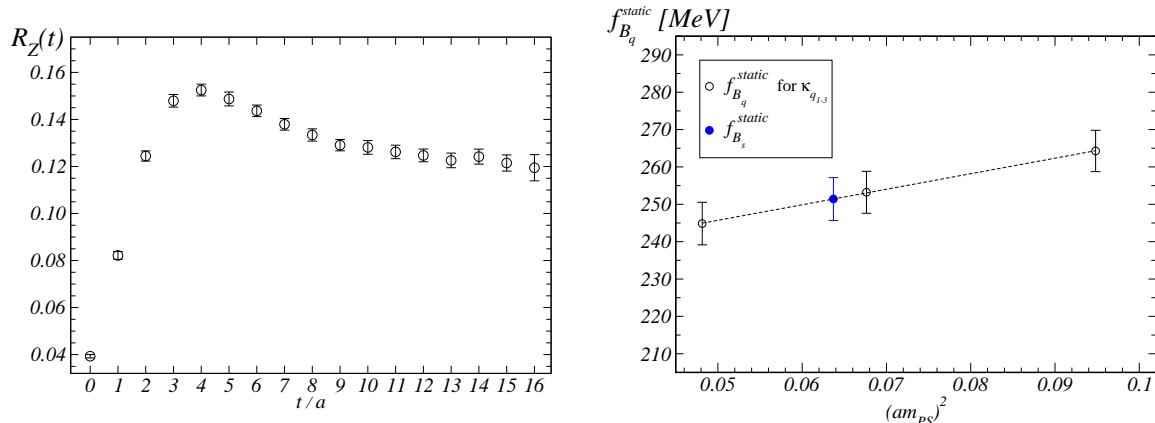


Figure 2: On the left, we illustrate the signal for the ratio $R_z(t)$ in the case $\kappa = 0.1344$. The fit of the plateau ($t/a \in [9; 13]$) to a constant gives \mathcal{Z}^L , which is then used to compute $f_{B_q}^{static}$ (see eq. (31)). The corresponding decay constants are shown in the right plot (empty circles). The result of the linear interpolation to the strange light quark, i.e. $f_{B_s}^{static}$, is marked by the filled circle. Notice that on the right plot only the statistical errors due to \mathcal{Z}_L are displayed.

which is independent of t_x (t_y is kept fixed). The same is true for the ratio (21) in which the denominator is composed of two correlators C_2 which are degenerate in this case so that the exponential t_x dependence explicitly cancels out, and one ends up with

$$R^{SS}(t_x) = \frac{C_{3ii}^{SS}(t_x)}{\mathcal{Z}_S^2 e^{-E_H^{SS} t_y}}. \quad (35)$$

In other words, the plateau for the ratio $R^{SS}(t_x)$ is equivalent to a plateau of $C_{3ii}^{SS}(t_x)$. A remarkable feature is that C_3 already develops a plateau at very a small time t_x . The physical interpretation could be that in the static limit, the *non-diagonal* matrix elements of the axial current simply vanish,

$$\langle H_k | A_i(t_x) | H_l^* \rangle_{k \neq l} \sim 0, \quad (36)$$

which implies that the t_x -dependence in the l.h.s. of eq. (34) vanishes as well when $k \neq l$. Note that this is the case in a quark model framework where the axial current reduces to a light quark spin operator. Since the spatial wave functions of the ground state and the excited states are orthogonal, the spin operator does verify eq. (36)².

As shown in eq. (21), the value of the bare coupling $\hat{g}_\infty^{(0)}$, is obtained from the fit of $R^{SS}(t_x)$ to a constant. We illustrate the signal for $R^{SS}(t_x)$ in fig. 3. The corresponding results are listed in table 2, where we also give the final results for $\hat{g}_\infty = Z_A^I \hat{g}_\infty^{(0)}$, for our set of light quarks (27). We also include the values of \hat{g}_∞ when the light quark is either the strange or the u/d quark. From the linear extrapolation to the chiral limit³, shown

²This statement is verified by our results using the static heavy quark. It is further corroborated by the matrix elements obtained by using the propagating heavy quark with a mass around the physical charm quark: we see that, as the heavy quark mass is increased, the three-point function $C_{3ii}^{SS}(0, t_x, t_y)$ begins to develop a plateau for smaller and smaller values of t_x .

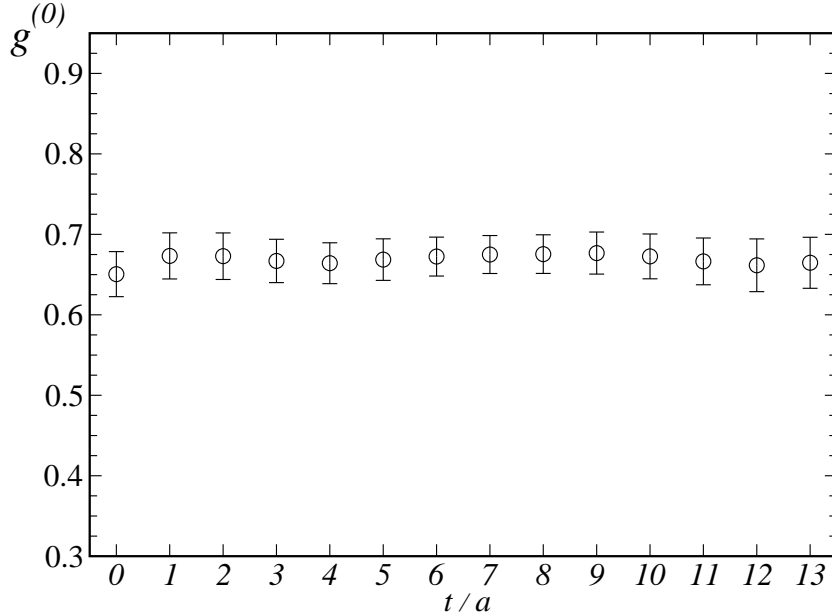


Figure 3: Signal for the ratio $R^{SS}(t_x)$ (see eq. (35)). Illustration is provided for $\kappa_{q_1} = 0.1344$. From the fit in $t/a \in [3, 10]$, we obtain the value of $\hat{g}_\infty^{(0)}$.

in fig. 4, we finally obtain,

$$\hat{g}_\infty = 0.48(3). \quad (37)$$

The results presented in this section have been obtained after having fixed $t_y = 13a < T/2$. This choice was made after we performed several simulations with $t_y/a \in [8, 13]$ and studied $R^{SS}(t_x)\mathcal{Z}_S^2$ for each t_y . We have checked that the result for $R^{SS}(t_x)\mathcal{Z}_S^2$ does not change as soon as t_y gets larger than $10a$. To separate the sources as far as possible we have chosen to fix t_y at $13a$.

4 Smearing, Fattening and Systematic uncertainties

As we already mentioned, to improve the statistical quality of the correlation functions computed with the static heavy quark action, we used the “fattening” procedure [17]. In addition, we use the smearing of the heavy–light interpolating fields [14], which helps isolating the lowest bound state at lower time separations. In this section we explain how the parameters of the smearing procedure were chosen (25) and show the benefits of using the “fat link” static heavy action instead of the standard Eichten–Hill one. After that discussion, we enumerate the sources of systematic uncertainties and estimate the related errors.

³We defer to subsection (4.3) the discussion of the validity of this procedure and of the uncertainties it induces.

	$\widehat{g}_\infty^{(0)}$	\widehat{g}_∞
static- q_1	0.67(2)	0.58(2)
static- q_2	0.65(3)	0.55(2)
static- q_3	0.63(3)	0.53(2)
static- s	0.64(3)	0.54(3)
static- u/d	0.59(3)	0.48(3)

Table 2: Bare and renormalized values of \widehat{g}_∞ . The time interval chosen to fit for a plateau in the ratio $R^{SS}(t)$ is $t/a \in [3, 10]$.

4.1 Smearing

The smearing procedure involves four parameters: R_{\max} , R_b , N_F and C (see eqs. (25-26)). The value of R_{\max} represents half the size of the hypercube where the smearing wave function lives and it is set to the maximal value allowed by the memory limitations. In our case, $R_{\max} = 5a$. The parameter R_b , which appears in the wave function $\phi(r) = e^{-r/R_b}$, is not fixed by any physical requirement other than improving the shape of the plateau for R_Z . The smeared-local correlators are much more sensitive to the variation of R_b than the smeared-smeared ones. In fig.5 we show the shape of $R_Z(t)$ for $R_b \in [1.0a, 4.0a]$. We see that if $R_b \geq 3.0a$, the value of $R_Z(t)$ on the plateau, and thus also the corresponding $f_{B_q}^{\text{static}}$, remains unchanged. The reason is that, as the wave function $\phi(r)$ lives in a typical volume of radius $R_{\max} = 5a$, the shape of the normalized wave function term $[(r + 1/2)^2 \phi(r)]$ in eq. (25) does not vary much when changing R_b in $3a - 5a$. Of course, all the physical quantities are built in such a way that, at the end, the effect of the normalization of $\phi(r)$ (i.e. the unwanted effect of the smearing) cancels. On the basis of these observations, we fix $R_b = 3a$.⁴

The remaining two parameters, C and N_F , enter in the fuzzing procedure (26). As far as C is concerned, it turns out that its value does not make any significant effect on our result. We varied its value in the range $C \in [0.8, 4.0]$, and the shape of $R_Z(t)$ does not change at all (of course, within our present statistical accuracy). On the other hand, the number of fuzzing iterations, N_F , is chosen to be $N_F = 5$. The effect of each iteration is to fuzz the spatial links by the gauge fields in the immediate neighborhood. By several iterations we can restore the effect of the wave function inside the volume of radius R_b , where $\phi(r)$ is supposed to live. As N_F iterations cover a volume of typical radius $(N_F + 1)^{1/2} a$, we should require $N_F \sim 8$ to fill a volume of radius $R_b = 3.0a$. It turns out, however, that for $N_F \geq 6$, the signal for R_Z begins to increase sharply: a large number of fuzzing iterations

⁴As a side remark, we note that the physical Compton wavelength of the D -mesons λ_D is given by the mass splitting between the D and the D_1 mesons masses. Its value, $\lambda_D = 2.2$ fm, is somewhat similar to $R_b = 3.0a \sim 2$ fm, that we use in our simulation.

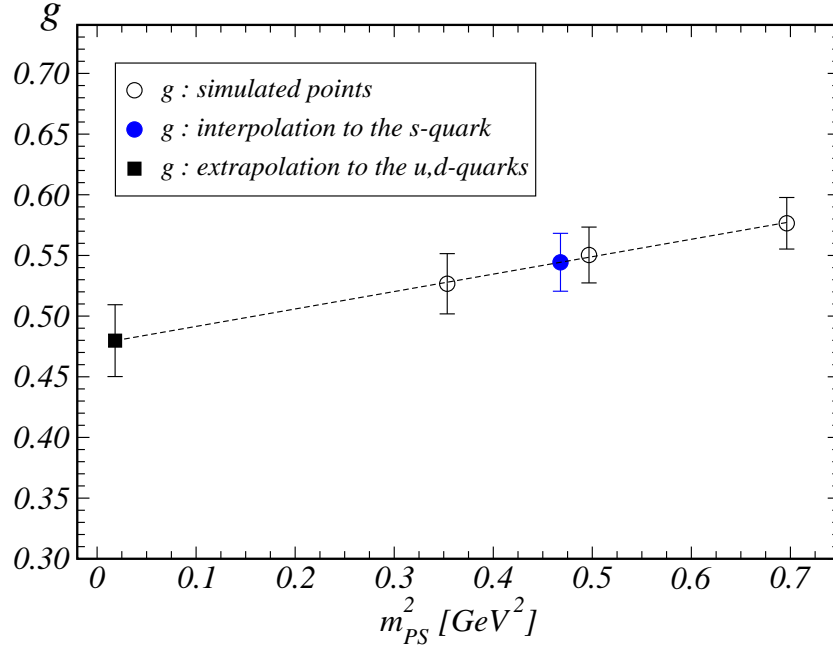


Figure 4: Linear extrapolation of \hat{g}_∞ to the chiral limit. The empty circles correspond to the simulated points whereas the filled symbols are the result of extra(inter)polation.

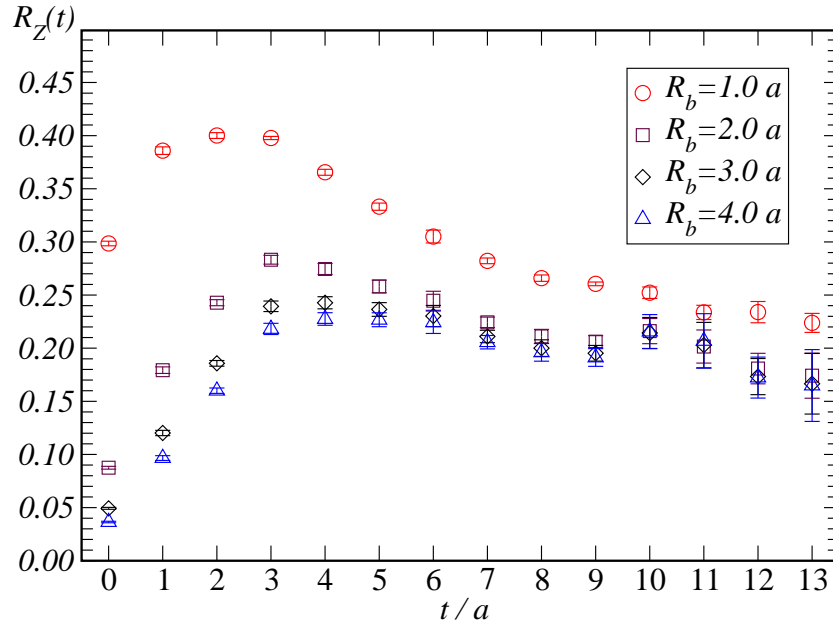


Figure 5: Effect on the ratio $R_Z(t)$ of the variation of R_b . For $R_b > 2.0 a$ the value of R_Z remains almost unchanged in the region $t \geq 7 a$. For this illustration we used the Eichten–Hill static heavy quark action, while the light Wilson quark κ is 0.1344.

destroy the quantum fluctuations as it was observed in the cooling procedures used to study instantons [21]. We checked that R_Z , and thus f_B^{static} , remain stable for $N_F \in [3, 5]$, and for the final simulation we chose $N_F = 5$.

4.2 Effect of “fattening” the static heavy quark propagator

In this subsection we show that replacing the link variables in the Eichten–Hill action by the “fat” ones (see eq. (24)), does make the plateau for the effective binding energies much larger, including a visible reduction of the statistical noise. In fact, after replacing $U_t \rightarrow U_t^{\text{fat}}$ in the Wilson line, the plateau gets extended to $t \sim 12a - 13a$, which is actually the upper limit ($T/2 = 14a$). From the comparison of the effective energy, eq. (29), obtained by using the “fat” Wilson line and of the standard one (i.e. without fattening), we can clearly see the improvement in the signal. This is illustrated in fig. 6, where in the case of “fat” Wilson line, the statistics is half what it was in the other case. This improvement is still more striking in the case where one uses the so-called Hyp-fattening (cf. refs. [22, 23]) instead of the standard one (see ref. [24]). We see that not only the plateau appears much clearer, but the signal remains longer in time. We also see that the two values of the effective binding energies are different, as expected, since the heavy quark lattice action was modified. In table 3, we compare the results obtained in both cases, i.e. with and without using the fattening procedure.

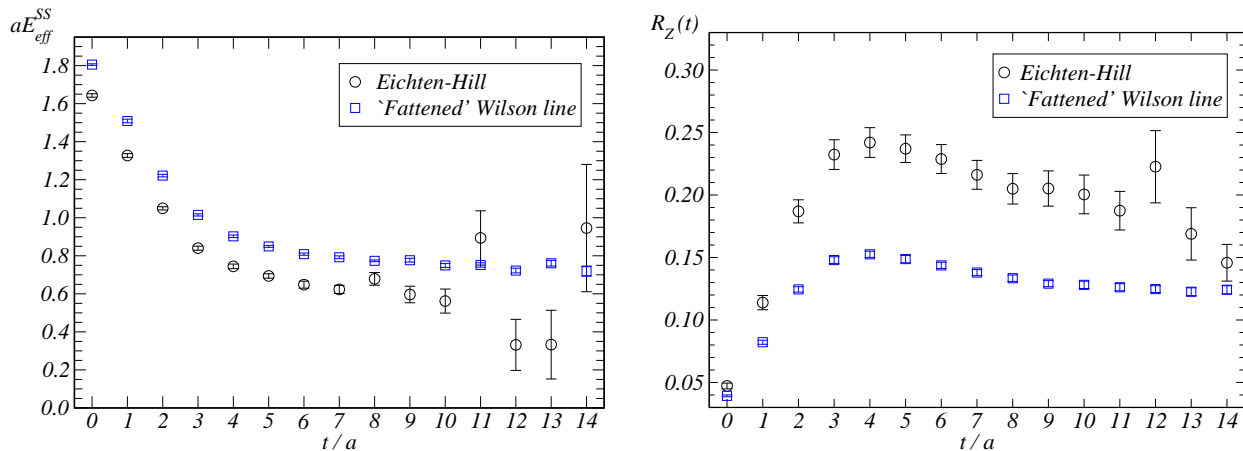


Figure 6: Comparison of the signals for the effective binding energies $E_{\text{eff}}^{\text{SS}}$ and Z^L when using either the usual Eichten–Hill action or its “fattened” version (see eq. (24)).

Before closing this subsection, we note also that, as far as the stability of the signal is concerned, the effect of replacing the standard Eichten–Hill action by the fat-link one is much more rewarding in the case of the heavy–light decay constant than for our \hat{g}_∞ . This is so because the operator whose matrix element is related to f_B^{static} includes a static quark, whereas the one related to \hat{g}_∞ does not. The fat link action however helps improving the statistical quality of the signal for \hat{g}_∞ . We note that, besides this improvement, the use of fattened links leads to a dramatic decrease of the value of $f_{B_s}^{\text{static}}$ with respect to what

	Eichten–Hill	‘Fattened’
$f_{B_s}^{\text{static}}$ [MeV]	410(56)	251(20)
\hat{g}_∞	0.58(8)	0.50(3)

Table 3: Values of $f_{B_s}^{\text{static}}$ and \hat{g}_∞ as computed from the usual Eichten–Hill static quark action and the new procedure with “fat” links. Parameters of both simulations are kept identical. In particular, to determine \hat{g}_∞ we have taken in this case $t_y = 10 a$.

had been found with the Eichten-Hill action. The fact that the plain EH formalism faces problems when trying to study f_B has been known for some time. In refs. [25, 27] it was shown that the smearing led to systematically lower values⁵. We show here that a similar effect results from the use of fattened links. In ref. [24] we show that the Hyp-fattening confirms fully the present results.

4.3 Systematic errors

- *Smearing:*

We combine in quadrature the effects of the variation of all the parameters of the smearing procedure on the resulting value for \hat{g}_∞ (see discussion in sec. 4.1). We estimate that systematics to be $\pm 15\%$.

- *Discretization errors:*

In our study we implemented the full $\mathcal{O}(a)$ improvement of the Wilson QCD action and the axial current. As we discussed in the text, the improvement of the bare axial current does not influence the value of \hat{g}_∞ . As for the renormalization constant, we used the non-perturbatively determined value, including the coefficient \tilde{b}_A , which ensures the elimination of the artifacts of $\mathcal{O}(a\rho)$.

Our main result is obtained from the simulation at $\beta = 6.2$. In order to study the $\mathcal{O}(a)$ effects, we also performed the simulations at $\beta = 6.1$ and $\beta = 6.0$, keeping the physical volume approximately the same and rescaling the smearing parameters. In fig. 7, we show the chiral behavior of \hat{g}_∞ , as computed in all three simulations. We see that both the results accessed directly from our simulations and those obtained after the linear extrapolation agree within the error bars. To give the reader a more quantitative insight into this effect, we collect in table 4 the results for \hat{g}_∞ and $f_{B_s}^{\text{static}}$ from all three simulations.

Since in this work we do not deal with propagating heavy quarks (which are usually the dominant source of discretization errors in the heavy–light meson observables), and since we do not observe any noticeable discretization error on \hat{g}_∞ from our

⁵We thank the anonymous referee for drawing those references to our attention.

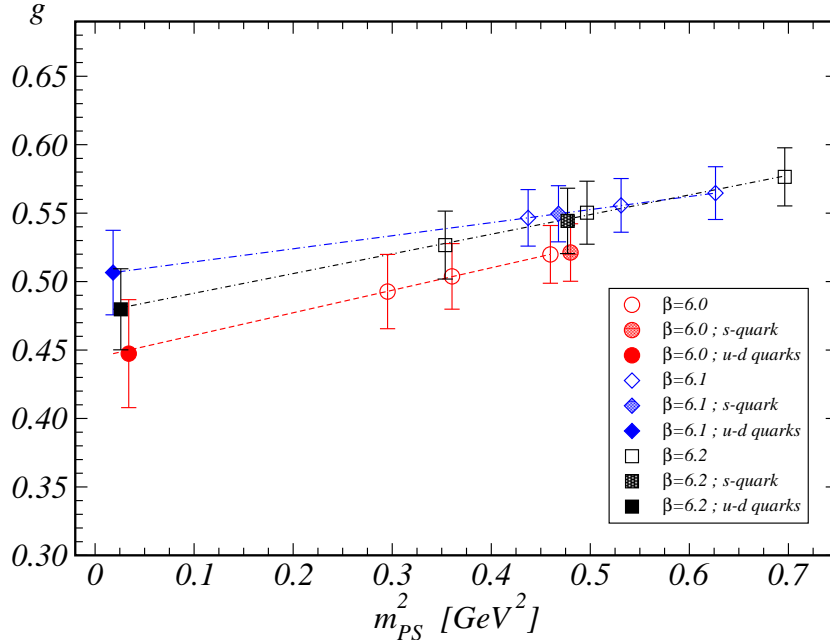


Figure 7: Comparison of the chiral extrapolations of \hat{g}_∞ from three simulations at $\beta = 6.0$, 6.1 and 6.2. The values extracted from these simulations are compatible within one standard deviation.

simulations at three different lattice spacings, we will not account for any extra discretization error in our overall systematic uncertainty⁶.

- *Finite volume:*

In this work we did not carry out a detailed study of the finite volume effects. Instead, we will rely on our previous study with the propagating heavy quark where the finite volume effects are estimated to be $\pm 6\%$ [4]. This uncertainty will be added in our overall systematic error estimate.

- *Chiral extrapolations:*

Since we have only three values for the bare light-quark masses, we cannot make a detailed study of the effect of the chiral extrapolation like the one we did in [4]. The values of \hat{g}_∞ that are directly accessed from our simulations follow a very smooth linear behavior when the value of the light quark mass is changed. The result (37) is obtained from the linear extrapolation. To that we will add an error of $\pm 15\%$, as estimated in our previous paper [4]. This error is considered symmetric for the reasons explained in detail in ref. [28]: the chiral logs in the full (unquenched) theory have a tendency to lower the value of the coupling \hat{g}_∞ , whereas those in the quenched theory do the opposite (increase the value \hat{g}_∞).

⁶Notice also that \hat{g}_∞ is dimensionless so that no discretization errors due to the conversion from the lattice to physical units arise.

β	6.0	6.1	6.2
$f_{B_s}^{\text{static}}$ [MeV]	250(35)	257(27)	251(20)
\hat{g}_∞	0.45(4)	0.51(3)	0.48(3)

Table 4: Values of $f_{B_s}^{\text{static}}$ and \hat{g}_∞ from three simulations at $\beta = 6.0, 6.1$ and 6.2 . Consistent results are found when comparing these studies.

After combining the above sources of systematic uncertainty in quadrature, we end up with 22% of error to the value given in eq. (37), i.e.

$$\hat{g}_\infty = 0.48 \pm 0.03 \pm 0.11 . \quad (38)$$

5 Heavy mass interpolation to the b -quark

We can now combine our static heavy quark result, \hat{g}_∞ , with those obtained in our previous study in which propagating heavy quarks with masses around the physical charm quark were used [4], to interpolate to the b -quark sector. For that purpose we use the spin-averaged mass of the heavy–light mesons, i.e.

$$\overline{m}_H = \frac{3m_V + m_P}{4} . \quad (39)$$

Motivated by the heavy quark symmetry, we fit our results to the linear and quadratic forms:

$$\hat{g}_Q = \hat{g}_\infty + \frac{a_1}{\overline{m}_H} , \quad (40)$$

$$\hat{g}_Q = \hat{g}_\infty + \frac{b_1}{\overline{m}_H} + \frac{b_2}{\overline{m}_H^2} . \quad (41)$$

These fits are shown in fig. 8, from which we read off the values at $1/\overline{m}_B = (5.314 \text{ GeV})^{-1}$, i.e. \hat{g}_b :

$$\hat{g}_b^{(lin)} = 0.55(4)(9), \quad \hat{g}_b^{(quad)} = 0.60(7)(9) . \quad (42)$$

As our final estimate we will take the average of the two, and add the difference in the overall systematics. Thus we have

$$\hat{g}_b = 0.58 \pm 0.06 \pm 0.10 , \quad (43)$$

which by means of eq. (1) gives

$$g_{B^*B\pi} = 47 \pm 5 \pm 8 . \quad (44)$$

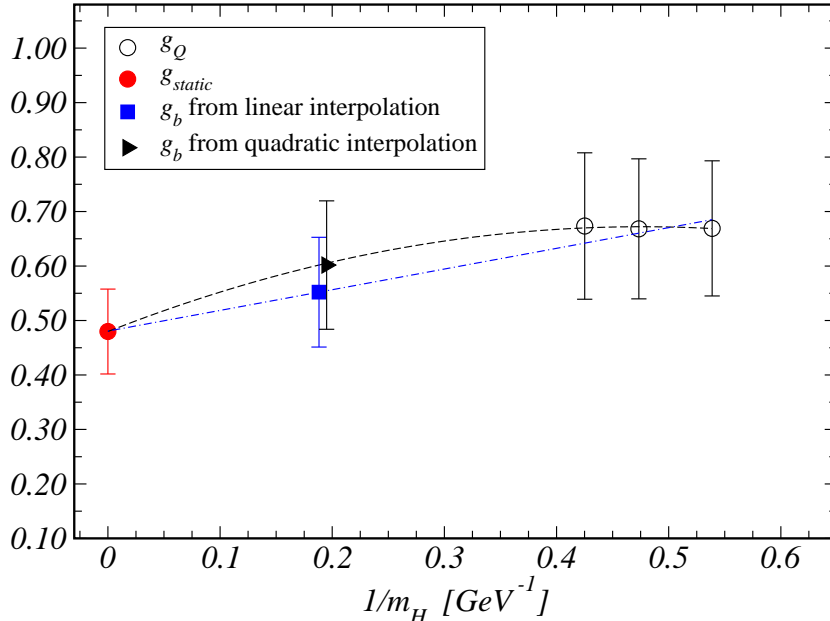


Figure 8: Heavy mass interpolation of the coupling \hat{g} to the B -meson sector, using heavy masses around the charm (empty circles) and our new result at the static limit (filled circle). The linear and quadratic fits defined in eqs. (40) and (41) give compatible results for \hat{g}_b (filled square and triangle).

6 Summary and conclusions

In this paper we made a study of \hat{g}_∞ , the coupling of the lowest-lying doublet of heavy-light mesons to a charged pion, in the infinitely heavy quark limit. The static heavy quark action used in this work is the Eichten and Hill one with fat-links, which ensures a better statistical quality of the correlation functions computed on the lattice. Our result, in the quenched approximation, is

$$\hat{g}_\infty = 0.48 \pm 0.03 \pm 0.11, \quad (45)$$

where the errors are statistical and systematic respectively. The most significant sources of systematic uncertainty are those related to the chiral extrapolation and to the smearing procedures used to suppress the contribution of the higher excited states in the relevant correlation functions.

That result is then combined with the ones reported in our previous work [4], in which we used propagating heavy quarks with masses close to the one of the physical charm quark. Interpolation to the b -quark sector leads to

$$\hat{g}_b = 0.58 \pm 0.06 \pm 0.10 \quad \text{and} \quad g_{B^* B \pi} = 47 \pm 5 \pm 8. \quad (46)$$

The quantities we have studied in this paper, \hat{g}_∞ and $g_{B^* B \pi}$, are very interesting because

- 1 they are of high phenomenological relevance,

- 2 they escape direct measurement,
- 3 their theoretical determinations are very widespread.

Still, as the attentive reader will have noticed, the errors remain larger large. Referring for instance to eq. (28) above, the statistical error is 6% and the systematic one 22%.

Concerning the statistical error a first factor is obviously the performance level of the available computing facilities. Since this is getting higher and higher rather fast and, at the same time, new computational techniques have been discovered which greatly improve the signal/noise ratio this source of uncertainty will probably be tamed very soon. Some of the systematic errors are no serious problems : most of the various renormalization and improvement constants we need have now been non perturbatively determined with an accuracy at the %-level. Note also that some of the (less well-known) heavy-light constants (e.g. $Z_{B_s}^{static}$) simply drop out of our computation. Some other ones are more serious :

The chiral extrapolation (which we have very roughly estimated to contribute by 15%) can be attacked on both the theoretical side (determination of the chiral logs) and the numerical one.

In this study we have used the static limit only as a limit point for our extrapolations from the finite-mass region. It is possible to go beyond this approach and to determine higher order $\frac{1}{M_Q}$ coefficients, which would allow a kind of “educated fit” and to decrease the theoretical uncertainties. This is part of an ambitious program which has been undertaken by the Alpha-group 3 years ago and is still under progress [29–32].

There remains the question of the unquenching. Its possibility while using the fattening procedures has been established (see ref. [33]) at least in the staggered-fermions case and probably with Wilson fermions too. This is one of the tasks we should undertake in the future.

These are just a few hints regarding what will have to be done now but it is impossible at present to outline any really sensible quantitative perspective regarding the time evolution in the near future of the various uncertainty factors we have just mentioned. Still, pursuing in the direction of a “pure QCD” determination of \hat{g} is clearly of primary importance.

Acknowledgement

We thank M. Della Morte, J. Reyes and A. Shindler for discussions and comments. The simulation was performed with the APE1000 located in the Centre de Ressources

Informatiques (Paris-Sud, Orsay) and purchased thanks to a funding from the Ministère de l'Education Nationale and the CNRS. This work was supported in part by the European Union Human Potential Program under contract HPRN-CT-2000-00/45, Hadrons/Lattice Phenomenology.

References

- [1] P. Colangelo and A. Khodjamirian, “*At the frontier of particle physics*”, vol. 3, 1495-1576; A. Khodjamirian, R. Ruckl, S. Weinzierl and O. I. Yakovlev, Phys. Lett. B **457** (1999) 245; F. S. Navarra, M. Nielsen and M. E. Bracco, Phys. Rev. D **65** (2002) 037502; A. Khodjamirian, eConf **C0304052** (2003) WG504.
- [2] D. Becirevic and A. Le Yaouanc, JHEP **9903** (1999) 021.
- [3] P. Singer, Acta Phys. Polon. B **30** (1999) 3849.
- [4] A. Abada *et al.*, Phys. Rev. D **66** (2002) 074504, and Nucl. Phys. Proc. Suppl. **119** (2003) 641.
- [5] P. Colangelo and F. De Fazio, Phys. Lett. B **532** (2002) 193; P. Colangelo, F. De Fazio and T. N. Pham, Phys. Lett. B **542** (2002) 71.
- [6] A. Abada *et al.*, Nucl. Phys. B **619**, 565 (2001); J.N. Simone, Nucl. Phys. Proc. Suppl. **119** (2003) 632.
- [7] S. R. Sharpe and Y. Zhang, Phys. Rev. D **53** (1996) 5125; A. S. Kronfeld and S. M. Ryan, Phys. Lett. B **543** (2002) 59; C. Bernard *et al.* [MILC Collaboration], Phys. Rev. D **66** (2002) 094501; D. Becirevic, S. Fajfer, S. Prelovsek and J. Zupan, Phys. Lett. B **563** (2003) 150; J. J. Sanz-Cillero, J. F. Donoghue and A. Ross, hep-ph/0305181.
- [8] M. B. Wise, Phys. Rev. D **45** (1992) 2188; T. M. Yan *et al.*, Phys. Rev. D **46** (1992) 1148 [Erratum-ibid. D **55** (1997) 5851]; G. Burdman and J. F. Donoghue, Phys. Lett. B **280** (1992) 287.
- [9] R. Casalbuoni, A. Deandrea, N. Di Bartolomeo, R. Gatto, F. Feruglio and G. Nardulli, Phys. Rept. **281** (1997) 145.
- [10] S. Ahmed *et al.* [CLEO Collaboration], Phys. Rev. Lett. **87** (2001) 251801; A. Anastassov *et al.*, Phys. Rev. D **65** (2002) 032003.
- [11] D. Becirevic, J. Charles, A. LeYaouanc, L. Oliver, O. Pène and J. C. Raynal, JHEP **0301** (2003) 009.
- [12] D. Melikhov and M. Beyer, Phys. Lett. B **452** (1999) 121; J. L. Goity and W. Roberts, Phys. Rev. D **64** (2001) 094007; M. Di Pierro and E. Eichten, Phys. Rev. D **64** (2001) 114004; W. Jaus, Phys. Rev. D **67** (2003) 094010.
- [13] G. M. de Divitiis *et al.* [UKQCD Collaboration], JHEP **9810** (1998) 010.
- [14] P. Boyle [UKQCD Collaboration], J. Comput. Phys. **179** (2002) 349.
- [15] E. Eichten and B. Hill, Phys. Lett. B **234** (1990) 511; A. Duncan *et al.*, Phys. Rev. D **51** (1995) 5101.

- [16] J. Heitger, M. Kurth and R. Sommer [ALPHA Collaboration], Nucl. Phys. B **669** (2003) 173
- [17] M. Della Morte *et al.* [ALPHA Collaboration], hep-lat/0307021.
- [18] M. Luscher, S. Sint, R. Sommer, P. Weisz and U. Wolff, Nucl. Phys. B **491** (1997) 323;
- [19] T. Bhattacharya, R. Gupta, W. J. Lee and S. R. Sharpe, Phys. Rev. D **63** (2001) 074505.
- [20] M. Luscher, S. Sint, R. Sommer and H. Wittig, Nucl. Phys. B **491** (1997) 344; D. Becirevic, V. Lubicz and G. Martinelli, Phys. Lett. B **524** (2002) 115.
- [21] M. Teper, Phys. Lett. B **162** (1985) 357; C. Michael and P. S. Spencer, Phys. Rev. D **52** (1995) 4691; P. Boucaud *et al.*, JHEP **0304** (2003) 005.
- [22] A. Hasenfratz and F. Knechtli, Phys. Rev. D **64** (2001) 034504
- [23] A. Hasenfratz, R. Hoffmann and F. Knechtli, Nucl. Phys. Proc. Suppl. **106**(2002) 418
- [24] A. Abada *et al.*, in preparation
- [25] G.P. Lepage, Nucl. Phys. Proc. Supp. **26** (1992) 51
- [26] S. Hashimoto and Y. Saeki, Nucl. Phys. Proc. Supp. **26** (1992) 381
- [27] C. Bernard, C.M. Heard, J. Labrenz and A. Soni, Nucl. Phys. Proc. Supp. **26** (1992) 384
- [28] D. Becirevic, S. Prelovsek and J. Zupan, Phys. Rev. D **67** (2003) 054010. and in preparation.
- [29] ALPHA, M. Kurth and R. Sommer, Nucl. Phys. B **597** (2001) 488.
- [30] ALPHA, J. Heitger and R. Sommer, Nucl. Phys. B Proc. Suppl. **106** (2002) 358.
- [31] R. Sommer, Nucl. Phys. B Proc. Suppl. **119** (2003) 185.
- [32] J. Heitger, M. Kurth and R. Sommer, Nucl. Phys. B Proc. Suppl. **119** (2003) 607
- [33] A. Hasenfratz, Nucl. Phys. B Proc. Suppl. **1119** (2003) 131